DIRECT MONTE-CARLO SIMULATION OF FIBER-INDUCED DRAG REDUCTION IN TURBULENT CHANNEL FLOW

Amin Moosaie
Fachgebiet Hydromechanik
Technische Universität München
Arcisstr. 21, 80333 München, Germany
a.moosaie@bv.tum.de

Michael Manhart
Fachgebiet Hydromechanik
Technische Universität München
Arcisstr. 21, 80333 München, Germany
m.manhart@bv.tum.de

ABSTRACT

We present a direct two-way coupled Monte-Carlo simulation of turbulent drag reduction by rigid fibers in a fully-developed channel flow. The numerical method is briefly described. Then, some results including the first- and second-order statistics of the velocity are presented and discussed.

INTRODUCTION

In this paper, we present the methodology and some selected results of the numerical simulation of drag reduction by rigid fibers in turbulent channel flow. The drag reducing property of polymer additives in turbulent flows, i.e. the Toms effect, has been known since 1948. Numerical investigation of this phenomenon has recently become feasible. Manhart performed a one-way coupled direct simulation of dilute Brownian fiber suspensions in turbulent channel flow (Manhart, 2003). Paschkewitz et al. (2004) studied the turbulent drag reduction by rigid fibers in channel flow using the moment approximation approach in a fully Eulerian framework. They, for example, found out that the drag reduction maximizes for non-Brownian fibers. Gillissen et al. (2007) performed two-way coupled moment approximation simulations as well as a direct computation based on the Fokker-Planck equation in turbulent channel flow based on a fully Eulerian framework. Their direct approach was limited to relatively strong Brownian motion (low Péclet numbers). For higher Péclet numbers, only results using moment closures have been available to date. In this work, we present a two-way coupled direct Monte-Carlo simulation strategy which is applicable to weak Brownian and even non-Brownian fibers for which the drag reduction is maximum. The turbulent flow field is computed using the direct numerical simulation (DNS) in an Eulerian framework. The fibers are treated in a Lagrangian framework. The Eulerian-Lagrangian two-way coupled simulation is presented in the following.

GOVERNING EQUATIONS

The isothermal incompressible flow of a non-Newtonian fluid is governed by the Navier-Stokes equations:

$$\rho \frac{\mathrm{D}\mathbf{U}}{\mathrm{D}t} = -\nabla p + \nabla \cdot \left(\tau^{\mathrm{N}} + \tau^{\mathrm{NN}} \right), \tag{1}$$

$$\nabla \cdot \mathbf{U} = 0, \tag{2}$$

in which ρ, $\mathbf{U}$ and p are the density of carrier fluid, velocity vector and pressure, respectively. The Newtonian stress τ^{N} is given by

$$\tau^{\mathrm{N}} = 2\mu\mathbf{D}, \quad \mathbf{D} = \tfrac{1}{2}\left(\nabla\mathbf{U} + \mathbf{U}\nabla\right), \tag{3}$$

where μ and $\mathbf{D}$ are the viscosity of the carrier fluid and the strain-rate tensor, respectively.

The non-Newtonian stress τ^{NN} is determined by the orientation distribution of the suspended fibers. The orientation of each fiber is described by its unit axial vector $\mathbf{n}$. The evolution of $\mathbf{n}$ depends on the background flow field and the intensity of rotary Brownian motion, and is governed by Jeffery's equation (Jeffery, 1922):

$$\frac{\mathrm{D}\mathbf{n}}{\mathrm{D}t} = \Omega \cdot \mathbf{n} + \kappa \left[\mathbf{D} \cdot \mathbf{n} - (\mathbf{n} \cdot \mathbf{D} \cdot \mathbf{n})\, \mathbf{n} \right] + \Gamma(t), \tag{4}$$

where Ω is the rotation-rate tensor, and $\Gamma(t)$ is the stochastic term representing the rotary Brownian motion. $\kappa = \left(r^2 - 1\right) / \left(r^2 + 1\right)$ is the fiber shape factor with r being the fiber aspect ratio. The non-Newtonian stress depends on $\langle \mathbf{nn} \rangle_\Psi$ and $\langle \mathbf{nnnn} \rangle_\Psi$, i.e. the second and fourth statistical moments of the fiber orientation distribution function via (Bren-

ner, 1974)

$$\begin{aligned}\tau^{\mathrm{NN}} = {} & 2\mu_0\mathbf{D} + \mu_1\mathbf{1}\left(\mathbf{D} : \langle\mathbf{nn}\rangle_\Psi\right) + \mu_2\mathbf{D} : \langle\mathbf{nnnn}\rangle_\Psi \\ & + 2\mu_3\left(\langle\mathbf{nn}\rangle_\Psi \cdot \mathbf{D} + \mathbf{D}\cdot\langle\mathbf{nn}\rangle_\Psi\right) \\ & + 2\mu_4 D_r\left(3\langle\mathbf{nn}\rangle_\Psi - \mathbf{1}\right),\end{aligned} \tag{5}$$

where $\mathbf{1}$ is the identity tensor. μ_i are the material coefficients given by Brenner (1974).

NUMERICAL METHODS

The numerical methods that are used to solve the system of equations described in section **??** are presented here. The Navier-Stokes equations (1) and (2) are solved on a non-equidistant Cartesian grid in an Eulerian framework using the projection method. The spatial discretization is carried out using second-order finite volume method. A low-storage third-order Runge-Kutta scheme is used for the time integration.

The fibers are treated by Lagrangian particle tracking. The Eulerian flow field is interpolated to Lagrangian points. Then, the Jeffery's equation (4) is integrated at the Lagrangian points. The stochastic term $\Gamma(t)$ is simulated by a Wiener process. The moments of orientation distribution function are computed by ensemble averaging. The Lagrangian field of the non-Newtonian stress is computed using (5). The Eulerian field of the non-Newtonian stress is then calculated by interpolation, and is supplied to the Navier-Stokes equation (1). The Lagrangian treatment of fibers offers the advantage that the Jeffery's equation is an ODE in the Lagrangian framework. The numerical method is explained in more details in (Manhart, 2003). The new feature of the present work is the two-way coupling that enables us to study the turbulent drag reducing effect of rigid fibers.

SIMULATION DETAILS

The fiber-induced drag reduction in turbulent channel flow at a shear Reynolds number $Re_\tau = 180$ is investigated. The computational domain is $\left(L_x, L_y, L_z\right) = (3\pi h, 2\pi h, 2h)$. The domain is discretized using 128^3 grid points. The grid is equidistant in the streamwise x and spanwise y directions. A non-equidistant grid in the wall-normal z direction is employed to account for the large gradients near the wall. Periodicity is assumed in x and y directions while the no-slip condition is applied at the walls in z direction. The flow is driven with a constant mean pressure gradient, and as a result, the bulk velocity is increased due to the fiber-induced drag reduction. The code is parallelized and the presented simulation has been performed on 128 processing elements.

The fiber aspect ratio and volume fraction are $r = 100$ and $\phi = 7.54 \times 10^{-3}$, respectively. The rotary Péclet number is $Pe = U_b/\left(hD_r\right) = 1000$ with U_b and D_r being the bulk velocity and the Brownian diffusivity, respectively. The number of Lagrangian particles is 6.5536×10^7. Each Lagrangian particle consists of 100 Monte-Carlo samples. This gives a total number of 6.5536×10^9 fibers for which the Jeffery's equation is solved.

RESULTS AND DISCUSSIONS

The fibrous flow simulation is performed using a fully developed Newtonian turbulent channel flow as the initial condition. After the introduction of fibers, the flow undergoes a transient regime and then a statistical steady state is reached. The statistical steady state used to calculate the turbulence statistics is shown in Fig. 1. The bulk velocity is increased by about 8.4%. This increase in the bulk velocity is better seen by looking at the mean velocity profile over the channel width as shown in Fig. 2. The mean velocity profiles of Newtonian and fibrous flows in inner coordinates are plotted in Fig. 3. The slope of the logarithmic region is similar to that of the Newtonian flow, but the intersection is greater which is an indication of the thickened viscous sublayer.

The Reynolds-averaged non-Newtonian Navier-Stokes equation yields that the sum of the mean viscous, Reynolds and non-Newtonian stresses equals to a linear function defined by the wall shear stress:

$$\mu\,\frac{\mathrm{d}\langle U\rangle}{\mathrm{d}z} - \rho\,\langle uw\rangle + \left\langle \tau_{xz}^{\mathrm{NN}} \right\rangle = \tau_w\,(1-z)\,. \tag{6}$$

Fulfilling this condition is a good test for the statistical convergence of the simulation. The shear stress balance of the Newtonian and fibrous flows is shown in Fig. 4. The fibrous flow has a smaller wall shear stress which is compensated by the non-Newtonian stress, the so-called stress deficit.

It is known that the fibers modify the turbulence intensities in the following way: the streamwise intensity increases while the spanwise and wall-normal intensities decrease. Our direct simulation verifies this result. The turbulence intensities are shown in Fig. 5. These modifications in turn augment the anisotropy property of the Reynolds stress tensor. In order to show this, the Lumley anisotropy map is plotted in Fig. 6. The main differences as compared to the Newtonian case can be summarized as the following. 1) The turbulence state is moved towards the one-component state at the wall. 2) The state in the buffer layer is also relocated towards the one-component state. 3) In the logarithmic region, the state slightly moves towards the axisymmetric turbulence. 4) The turbulence is less isotropic at the channel centerline. These observations are in line with the findings of Frohnapfel *et al.* (2007).

CONCLUSIONS

In this paper, a methodology for two-way coupled direct Monte-Carlo simulation of turbulent drag reduction by rigid fibers is presented. The change in bulk velocity, the mean velocity profile, the shear stress balance, the turbulence intensities and the Lumley anisotropy map are presented and discussed. The proposed method does not require a closure model as is the case in moment approximation approach. Moreover, it is well suited to high *Pe* where maximum drag reduction takes place and the direct solutions based on the Fokker-Planck equation are computationally expensive.

ACKNOWLEDGMENTS

This work is financially supported by the International Graduate School of Science and Engineering (IGSSE) at the

Technische Universität München. Computational resources have been provided by the Leibniz supercomputing center (LRZ) of the Bavarian Academy of Sciences in Munich.

REFERENCES

[1] Brenner, H., 1974, "Rheology of a Dilute Suspension of Axisymmetric Brownian Particles", Int. J. Multiphase Flow, Vol. 1, pp. 195-341.

[2] Frohnapfel, B., Lammers, P., Jovanovic, J., Durst, F., 2007, "Interpretation of the Mechanism Associated with Turbulent Drag Reduction in Terms of Anisotropy Invariants", J. Fluid Mech., Vol. 577, pp. 457-466.

[3] Gillissen, J.J.J., Boersma, B.J., Mortensen, P.H. and Andersson, H.I., 2007, "On the Performance of the Moment Approximation for the Numerical Computation of Fiber Stress in Turbulent Channel Flow", Phys. Fluids, Vol. 19, pp. 035102.

[4] Jeffery, G., 1922, "The Motion of Ellipsoidal Particles Immersed in a Viscous Fluid", Proc. R. Soc. Lond. A, Vol. 102, pp. 161-179.

[5] Manhart, M., 2003, "Rheology of Suspensions of Rigid-Rod Like Particles in Turbulent Channel Flow" J. Non-Newtonian Fluid Mech., Vol. 112, pp. 269-293.

[6] Paschkewitz, J.S., Dubief, Y., Dimitropoulos, C.D., Shaqfeh, E.S.G. and P. Moin, 2004, "Numerical Simulation of Turbulent Drag Reduction Using Rigid Fibres", J. Fluid Mech., Vol. 518, pp. 281-317.

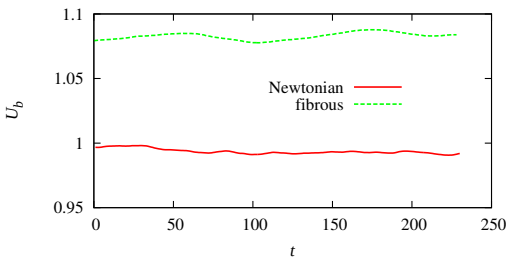

Figure 1. Bulk velocity of Newtonian and drag-reduced flows versus time. Shown is the time span used for averaging.

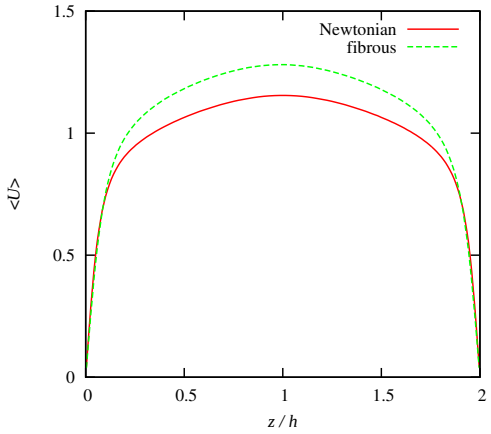

Figure 2. Mean velocity profile of Newtonian and drag-reduced flows versus channel width.

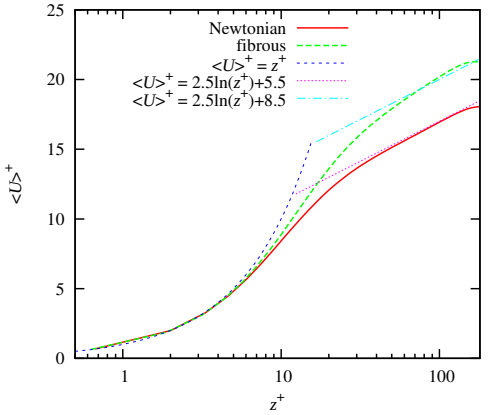

Figure 3. Mean velocity profile of Newtonian and drag-reduced flows in inner scaling versus channel width.

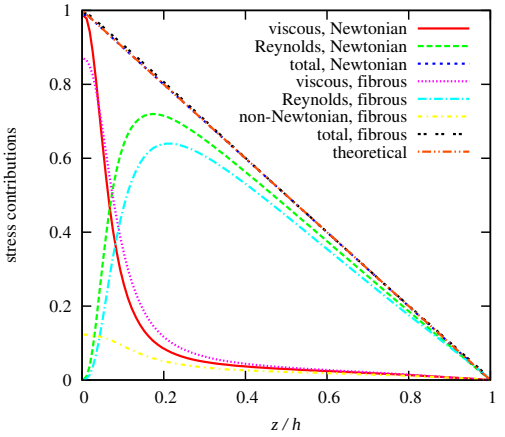

Figure 4. Shear stress balance of Newtonian and fibrous flows versus channel width.

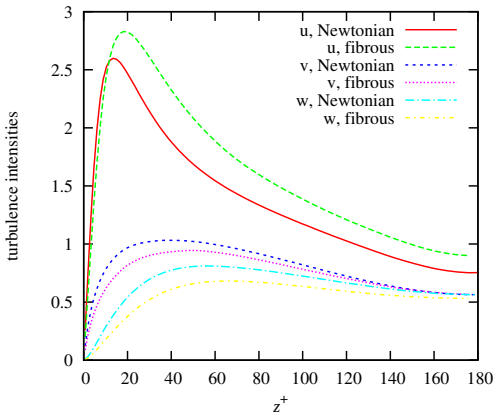

Figure 5. Turbulence intensities of Newtonian and drag-reduced flows versus channel width.

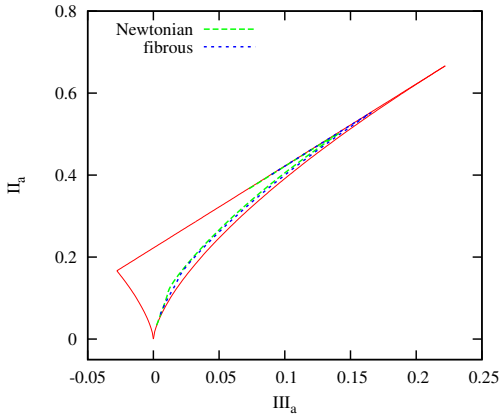

Figure 6. Lumley anisotropy map of Newtonian and fibrous flows.